Internal thermal stress distribution in InGaAsP/InP lasers

J. M. Liu, Y. C. Chen, and S. F. Wayne
GTE Laboratories, Inc., 40 Sylvan Road, Waltham, Massachusetts 02254

(Received 23 June 1986; accepted for publication 12 August 1986)

The two-dimensional distribution of the internal thermal stress in the active layer of a buried heterostructure InGaAsP/InP laser is calculated with the finite-element method for active regions of both rectangular and crescent shapes. The shape and the finite width of the stripe cause nonuniform distribution of the thermal stress in the active layer. The results show different distributions for these two shapes, particularly near the edges of the active regions. Large stress and stress gradient are found around the tips of the crescent, which may imply problems such as defects and mode instability in real devices.

Double heterostructure semiconductor lasers usually consist of a thin active layer sandwiched between two cladding layers on a thick substrate. In these structures, internal thermal stresses generally result from the lattice mismatch and the differential thermal expansion coefficients between layers of different compositions.[1-5] In the AlGaAs/GaAs laser structures, most of the internal stresses reside in the AlGaAs cladding layers. Except for AlGaAs/GaAs of very short wavelengths,[3] the thermal stress in the active layer is largely offset by the thick GaAs substrate whose composition is close to that of the active layer. The stress is usually compressive along the junction plane[5] and is about one order of magnitude smaller than that in the cladding layers. It has been pointed out[2] that active layers under compressive stresses are more resistant to degradation phenomena than those under tensile stresses. Moreover, the compressive stress in the active layer tends to enhance the normally operating TE (transverse electric) mode of an AlGaAs/GaAs laser.[6]

The situation is very different for the InGaAsP/InP lasers, in which a thin InGaAsP active layer is sandwiched between InP cladding layers on a thick InP substrate. Under usual liquid phase epitaxy (LPE) growth conditions, the stress in the active layer tends to be tensile along the junction plane at room temperature because InGaAsP has a larger thermal expansion coefficient than InP. This tensile stress in the active layer can promote competition between TE and TM (transverse magnetic) laser modes[6] in addition to many other undesirable effects. We have previously studied[6,7] the effects of the internal thermal stresses on the polarization behavior of InGaAsP/InP lasers. The stress in the active InGaAsP layer caused by thermal strain in the multilayer structure was calculated[5,6] with the generalized formula[4] for a simplified one-dimensional N-layer structure.

However, the realistic structure of the popular buried heterostructure InGaAsP/InP laser consists of a thin, narrow InGaAsP stripe of rectangular or crescent shape buried in the InP surroundings. The shape and the finite width of the stripe may cause nonuniform distribution of the thermal stress in the active layer. This problem is studied in the present report. The two-dimensional distribution of the internal thermal stress in the active layer of a buried heterostructure InGaAsP/InP laser is calculated with the finite-element method (Gifts code) for both rectangular and crescent shapes. The results show very different distributions for these two shapes.

In our calculations, we assume an $In_{0.74}Ga_{0.26}As_{0.6}P_{0.4}$ active layer (for $\lambda = 1.3\,\mu m$) of $2\,\mu m$ width $\times\, 0.2\,\mu m$ thickness buried in InP cladding layers of $1\,\mu m$ thickness grown on a (100) InP substrate of $80\,\mu m$ thickness. The cavity length and the width of the substrate are on the order of 200 μm. To facilitate the analysis for the thermal stress induced by the differential thermal expansion, the structure is as-

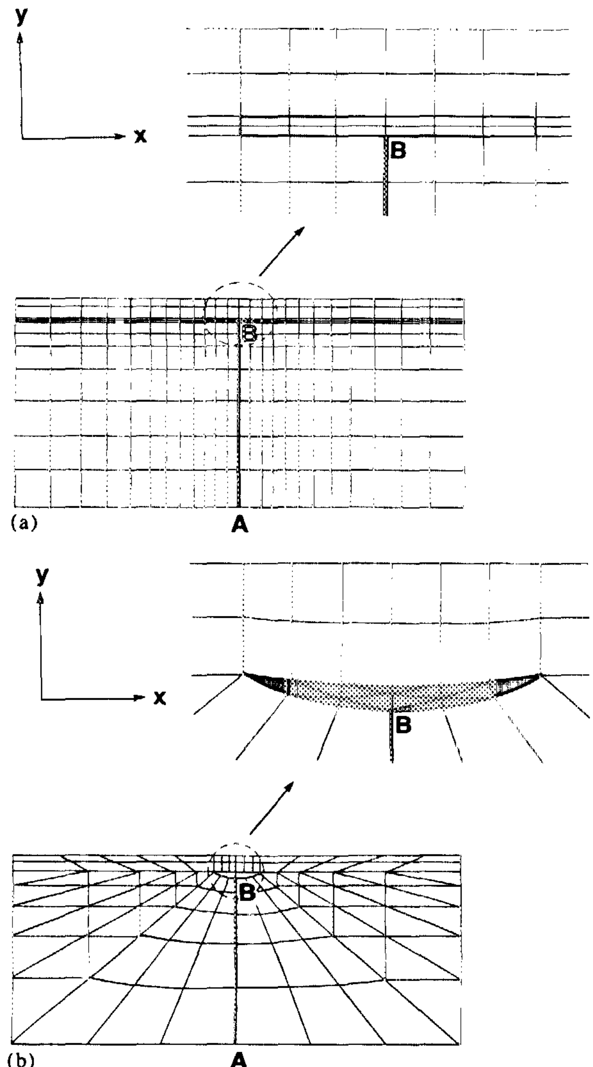

FIG. 1. Biased finite-element meshes for the laser structures with (a) rectangular and (b) crescent active regions. The shaded areas in the enlarged portions show the details of the active regions.

 © 1986 American Institute of Physics

Downloaded 19 Sep 2003 to 146.95.52.13. Redistribution subject to AIP license or copyright, see http://ojps.aip.org/aplo/aplcr.jsp

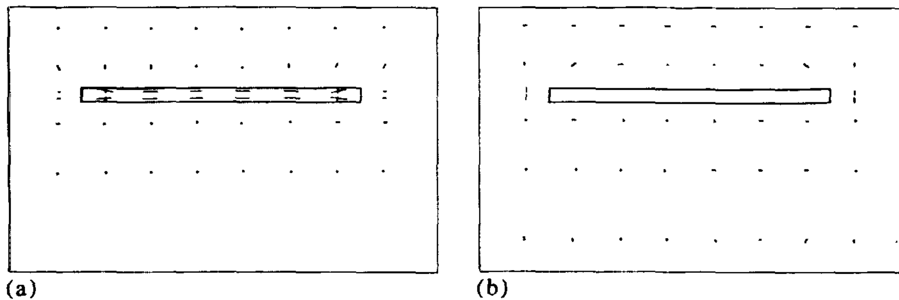

FIG. 2. Distribution of the principal (a) tensile and (b) compressive stresses in the laser structure with a rectangular active region.

sumed to be grown perfectly lattice matched at the 650 °C growth temperature and the internal thermal stress in the active layer at 20 °C is calculated. The case for perfect lattice matching at other temperatures can be extrapolated or interpolated through a linear relation. The result of the finite-element calculation depends critically on the choice of proper boundary conditions. The boundary conditions are such that points on the line of symmetry, *AB*, in Figs. 1(a) and 1(b), are allowed to move only vertically with respect to one fixed point, such as *A* or *B*, on the line. All other points in the LPE-grown structure then move freely according to the law of thermal expansion without any external mechanical constraint or any internal dislocation. In order to examine the validity of these boundary conditions, the simplified multilayer InGaAsP/InP and AlGaAs/GaAs structures analyzed in Ref. 5 were analyzed with the finite-element method with these boundary conditions and were compared with the results described therein. The comparison showed differences in the results within 5%, which probably could be accounted for by the fact that in the calculations in Ref. 5 the same Young's modulus and Poisson's ratio were taken for the layers of different compositions for simplification of calculation.

For quick convergence of the numerical calculation, biased finite-element meshes were created for the structures, as are shown schematically in Figs. 1(a) and 1(b). The thermal expansion coefficients[5] for InP and $In_{0.74}Ga_{0.26}As_{0.6}P_{0.4}$ are $\alpha_1 = 4.56\times10^{-6}/°C$ and $\alpha_2 = 5.42\times10^{-6}/°C$, respectively. The Young's moduli[8] are $E_1 = 6.04\times10^{11}$ dyn/cm^2 and $E_2 = 6.48\times10^{11}$ dyn/cm^2, respectively. The Poisson's ratios[8] are $\nu_1 = 0.36$ and $\nu_2 = 0.342$, respectively.

Figures 2 and 3 show the overall distribution of the principal stresses in the active regions of rectangular and crescent shapes, respectively. As expected, the active regions are completely free of compressive stresses. The tensile stresses are parallel to the junction plane except at the corners where directions of the tensile stresses change slightly due to the change in geometry. In order to obtain greater resolution in and around the active region, further computations were made with a highly refined mesh intended to minimize edge effects. It should be mentioned that the values for the stresses have been calculated in a local, rather than global, coordinate system, thus allowing for comparisons of material mismatch.

Figure 4(a) shows the detailed distribution of the normal and shear tensile stresses for active regions of both rectangular and crescent shapes from the center to the edge along a horizontal line in the middle of each active region. For active regions of both shapes, the tensile stresses are predominantly normal stresses in the horizontal (x) direction, i.e., along the junction plane, because of the elongated geometry of the active regions. For the rectangular shape, the shear stress (xy) is virtually nonexistent. For the crescent shape, there is some shear stress existing across the whole active region, although it is small compared to the horizontal normal stress (xx). It is very interesting to notice the difference between the normal stress distributions in rectangular and crescent active regions. The normal stresses in a rectangular active region are quite uniform across the whole area. Only near the edges does the horizontal normal stress (xx) start to decrease while the vertical normal stress (yy) increases substantially. In contrast, the horizontal normal stress in a crescent active region first increases as one approaches the corners, while the vertical normal stress remains small. In both cases, the stress falls rapidly to a negligible level within a short distance outside the active region. However, the distance over which the stress changes is much larger for a rectangular shape. As a result, the crescent shape has a much more nonuniform stress distribution and a much

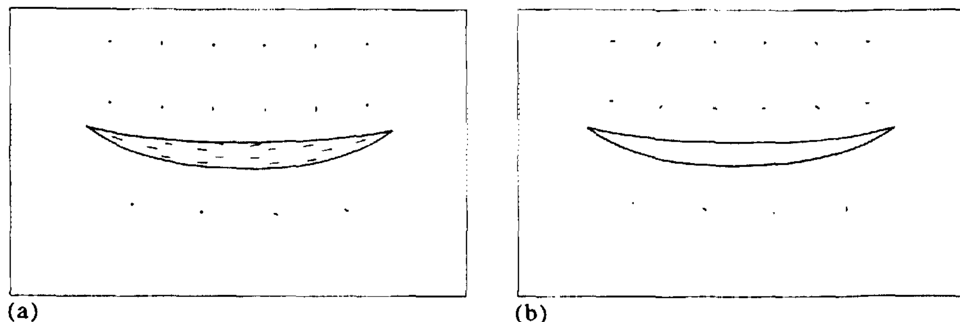

FIG. 3. Distribution of the principal (a) tensile and (b) compressive stresses in the laser structure with a crescent active region.

Downloaded 19 Sep 2003 to 146.95.52.13. Redistribution subject to AIP license or copyright, see http://ojps.aip.org/aplo/aplcr.jsp

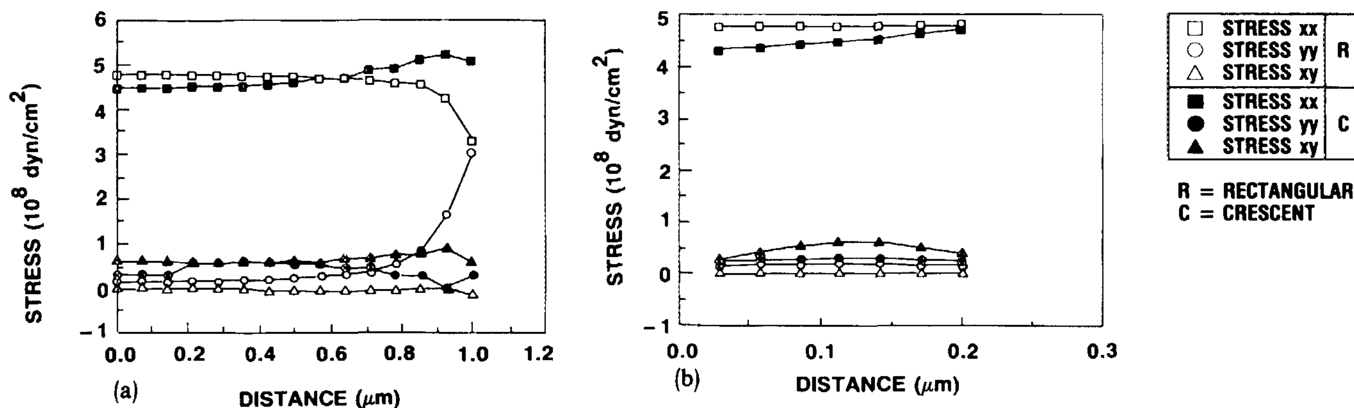

FIG. 4. Detailed distribution of normal (xx and yy) and shear (xy) tensile stresses at room temperature for active regions of both shapes which are grown perfectly lattice matched at 650 °C. (a) From center to edge along a horizontal line in the middle of each active region. Distance is measured from the center. (b) From bottom to top along the vertical line of symmetry of each active region. Distance is measured from the bottom.

larger stress gradient at the corners than the rectangular shape. The sharp tips of the crescent behave as singular points where large stress and stress gradient exist. The stress distributions for both shapes from the bottom to the top along the vertical line of symmetry of each active region are shown in Fig. 4(b). For a rectangular active region, the stress is constant along this line, while again there is some nonuniformity in the stress distribution in a crescent active region.

In these calculations, the layers were assumed to be grown perfectly lattice matched at the 650 °C LPE growth temperature. Nakajima *et al.*[9] and Yamazaki *et al.*[10] have shown that misfit dislocation-free InGaAsP/InP layers should be grown under the conditions that the InGaAsP layer is perfectly lattice matched to InP or is slightly under a tensile stress (negative lattice mismatch) at the growth temperature, rather than under the conditions that the layers will be lattice matched at room temperature. It is obvious that even when the layers were grown dislocation-free,[9,10] additional stress could still be introduced by lattice mismatch between the layers during LPE growth. Therefore, our analyses discussed above address only the distribution of the internal thermal stresses generated from the differential thermal expansion. The actual stress distribution is subject to changes in the initial growth conditions which depend on individual cases. However, it can be observed from our calculations that if the layers are lattice matched during growth, the thermal stress on the order of 5×10^8 dyn/cm^2 at room temperature will introduce a negative lattice mismatch smaller than 5×10^{-4} at the center of the active region. This amount of negative lattice mismatch is not sufficient to cause dislocations.[9,10] Also, the thermal stress does not appear to be a problem on the edges and corners of the active region. For laser structures of longer wavelengths, such as $In_{0.53}Ga_{0.47}As$/InP, the thermal stress can be as large as 8×10^8 dyn/cm^2 at room temperature. It is very desirable to grow the layers under lattice-matching conditions to prevent dislocations.[9,10] Temkin *et al.*[11] have reported that the growth of long wavelength buried crescent InGaAsP/InP lasers, such as 1.55 and 1.62 μm, is very difficult and nonreproducible primarily because of the competition of (100) growth and (111)*B* growth which have very different growth kinetics. In this case, internal strain can also be introduced by inhomogeneous growth of the active layer.[11]

The finite-element calculations can be extended to include stresses induced by external sources such as the oxide layers, the metallization, the die-bonding material, and the heat sink. Koyama *et al.*[12] have previously employed the finite-element method to calculate the stress distribution in a GaAs diode induced by the Si submount and the Cu heat sink block. They have made the assumption that the Au solder layers located at the laser/submount and submount/heat sink block interfaces can be neglected in the stress calculations.[12] In fact, although these layers are very thin, they have very substantial influence on the stress distribution in the structure.[13] Because they are thin compared to their neighbors, the stress in these layers caused by the differential thermal expansion of their neighbors can be very large. However, the metallic solder materials typically have very low yield stresses on the order of 10^9 dyn/cm^2. Plastic deformation in these thin layers will occur if the thermal stress increases beyond their yield stresses.[13] In this case, the solder layers tend to act as buffers between layers of very different materials. To simulate the whole structure with the finite-element method, these effects should be carefully taken into account because meaningful results from the finite-element calculations depend critically on the choice of proper boundary conditions.

[1]F. K. Reinhart and R. A. Logan, J. Appl. Phys. **44**, 3171 (1973).
[2]G. H. Olsen and M. Ettenberg, J. Appl. Phys. **48**, 2543 (1977).
[3]H. Shimizu, K. Itoh, M. Wada, T. Sugino, and I. Teramoto, IEEE J. Quantum Electron. **QE-17**, 763 (1981).
[4]Z. C. Feng and H. D. Liu, J. Appl. Phys. **54**, 83 (1983).
[5]J. M. Liu and Y. C. Chen, IEEE J. Quantum Electron. **QE-21**, 271 (1985).
[6]Y. C. Chen and J. M. Liu, Appl. Phys. Lett. **45**, 731 (1984).
[7]Y. C. Chen and J. M. Liu, Appl. Phys. Lett. **45**, 604 (1984).
[8]S. Adachi, J. Appl. Phys. **53**, 8775 (1982).
[9]N. Nakajima, S. Yamazaki, S. Komiya, and K. Akita, J. Appl. Phys. **52**, 4575 (1981).
[10]S. Yamazaki, Y. Kishi, K. Nakajima, A. Yamaguchi, and K. Akita, J. Appl. Phys. **53**, 4761 (1982).
[11]H. Temkin, R. A. Logan, and J. P. Van der Ziel, Appl. Phys. Lett. **44**, 160 (1984).
[12]H. Koyama, T. Nishioka, K. Isshiki, N. Namizaki, and S. Kawazu, Appl. Phys. Lett. **43**, 733 (1983).
[13]G. E. Henein and W. R. Wagner, J. Appl. Phys. **54**, 6395 (1983).

Downloaded 19 Sep 2003 to 146.95.52.13. Redistribution subject to AIP license or copyright, see http://ojps.aip.org/aplo/aplcr.jsp